

Rate constants for the reactions of OH radicals with a series of 1,4-hydroxyketones

Jillian Baker^a, Janet Arey^b, Roger Atkinson^{b,c,*}

^a Environmental Sciences Graduate Program and Air Pollution Research Center, University of California, Riverside, CA 92521, USA

^b Air Pollution Research Center and Department of Environmental Sciences, University of California, Riverside, CA 92521, USA

^c Department of Chemistry, Air Pollution Research Center, University of California, Riverside, CA 92521, USA

Received 13 July 2005; received in revised form 27 July 2005; accepted 27 July 2005

Available online 1 September 2005

Abstract

A series of C₅–C₈ 1,4-hydroxyketones were generated in situ from the OH radical-initiated reactions of their *n*-alkane precursors. By investigating the time-concentration behavior of these hydroxyketones during the reactions, rate constants for the reactions of OH radicals with the hydroxyketones at 298 ± 2 K were determined relative to the rate constant for the reaction of OH radicals with the parent *n*-alkane. The hydroxyketones were monitored by Solid Phase MicroExtraction, using fibers pre-coated with *O*-(2,3,4,5,6-pentafluorobenzyl)hydroxylamine for on-fiber derivatization of carbonyl compounds, with analysis of their oxime derivatives by gas chromatography with flame ionization detection. Initial experiments at ≤5% relative humidity showed that 5-hydroxy-2-hexanone and 6-hydroxy-3-hexanone (formed from *n*-hexane) disappeared more rapidly than could be accounted for by reaction with OH radicals, suggesting that these hydroxyketones were also undergoing cyclization with loss of water to form alkyl-substituted 4,5-dihydrofurans. Accordingly, all further experiments were carried out at 50 ± 5% relative humidity, and the enhanced disappearance of hydroxyketones was markedly reduced (but was still evident for the hydroxyoctanones formed from *n*-octane). The rate constants derived for the 1,4-hydroxyketones formed from *n*-pentane through *n*-octane were in the range (1.5–2.4) × 10⁻¹¹ cm³ molecule⁻¹ s⁻¹, consistent with rate constants estimated using the structure–reactivity method of Kwok and Atkinson [E.S.C. Kwok, R. Atkinson, *Atmos. Environ.* 29 (1995) 1685–1695].

© 2005 Elsevier B.V. All rights reserved.

Keywords: 1,4-Hydroxyketones; Hydroxyl radical; Kinetics; Atmospheric reactions

1. Introduction

Alkanes are important constituents of gasoline and vehicle exhaust [1] and account for ~50% of the non-methane volatile organic compounds observed in ambient air in urban areas [2]. In the atmosphere, alkanes react primarily with OH radicals [3], leading in the presence of NO to the formation of alkyl nitrates, carbonyls, 1,4-hydroxyalkyl nitrates and 1,4-hydroxycarbonyls [4–8], with formation of 1,4-hydroxycarbonyls accounting for >50% of the products from the ≥C₆ *n*-alkanes [8]. Reisen et al. [8] identified and quantified 5-hydroxy-2-pentanone and 4-hydroxypentanal from

the *n*-pentane reaction; 5-hydroxy-2-hexanone, 6-hydroxy-3-hexanone and 4-hydroxyhexanal from the *n*-hexane reaction; 5-hydroxy-2-heptanone, 6-hydroxy-3-heptanone, 1-hydroxy-4-heptanone and 4-hydroxyheptanal from the *n*-heptane reaction; and 5-hydroxy-2-octanone, 6-hydroxy-3-octanone, 7-hydroxy-4-octanone and 4-hydroxyoctanal from the *n*-octane reaction. A detailed reaction mechanism for the atmospheric reactions of the 2-hexyl radical, one of the hexyl radicals formed after H-atom abstraction from *n*-hexane, leading to the formation of 5-hydroxy-2-hexanone and other observed and potential products, is shown elsewhere [7]. Previous studies of 5-hydroxy-2-pentanone, the only commercially available 1,4-hydroxycarbonyl, have shown that it reacts with OH radicals with a room temperature rate constant of (1.6 ± 0.4) × 10⁻¹¹ cm³ molecule⁻¹ s⁻¹ [9] and that

* Corresponding author. Tel.: +1 951 827 4191.

E-mail address: ratkins@mail.ucr.edu (R. Atkinson).

in reaction chambers in dry air or N₂ it converts (via cyclization and loss of water) to 4,5-dihydro-2-methylfuran [10,11] which is highly reactive towards OH and NO₃ radicals and O₃ [11].

In this work, we have generated the C₅–C₈ 1,4-hydroxycarbonyls 5-hydroxy-2-pentanone [CH₃C(O)CH₂CH₂CH₂OH], 5-hydroxy-2-hexanone [CH₃C(O)CH₂CH₂CH(OH)CH₂CH₃], 6-hydroxy-3-hexanone [CH₃CH₂C(O)CH₂CH₂CH₂OH], 5-hydroxy-2-heptanone [CH₃C(O)CH₂CH₂CH(OH)CH₂CH₃], 6-hydroxy-3-heptanone [CH₃CH₂C(O)CH₂CH₂CH(OH)CH₂CH₃], 1-hydroxy-4-heptanone [HOCH₂CH₂CH₂C(O)CH₂CH₂CH₃], 5-hydroxy-2-octanone [CH₃C(O)CH₂CH₂CH(OH)CH₂CH₂CH₃], 6-hydroxy-3-octanone [CH₃CH₂C(O)CH₂CH₂CH(OH)CH₂CH₃] and 7-hydroxy-4-octanone [CH₃CH₂CH₂C(O)CH₂CH₂CH(OH)CH₃] in situ from their *n*-alkane precursors and investigated their reactions with OH radicals. Because 1,4-hydroxycarbonyls do not elute from gas chromatographic columns without prior derivatization [4,7], we used Solid Phase MicroExtraction (SPME) fibers pre-coated with *O*-(2,3,4,5,6-pentafluorobenzyl)hydroxylamine (PFBHA) to allow in situ derivatization of the 1,4-hydroxycarbonyls for analysis as their oxime derivatives by gas chromatography with flame ionization detection (GC-FID) [8,9].

2. Experimental methods

Experiments were carried out in a ~7000-l Teflon chamber at 298 ± 2 K and 740 Torr total pressure of purified air at ≤5% and (in the majority of the experiments) 50 ± 5% relative humidity. The chamber is equipped with a Teflon-coated fan to ensure rapid mixing of the reactants during their introduction into the chamber, and has two parallel banks of blacklamps for irradiation. Hydroxyl (OH) radicals were generated by the photolysis of methyl nitrite (CH₃ONO) in air at wavelengths >300 nm [12], and NO was added to the reactant mixtures to suppress (at least in the early stages of the reactions) the formation of O₃, and hence of NO₃ radicals [12].

The initial reactant concentrations (in molecule cm⁻³) were: CH₃ONO and NO, ~4.8 × 10¹³ each; *n*-pentane, ~2.3 × 10¹³, *n*-hexane, ~1.1 × 10¹³, *n*-heptane, ~1.3 × 10¹³ or *n*-octane, ~1.5 × 10¹³. The methyl nitrite concentrations were purposefully kept relatively low in order to avoid the formation of high concentrations of HCHO (from photolysis of methyl nitrite), which would be derivatized and it was thought might lead to depletion of the derivatizing agent, and hence to a decreasing response for the hydroxycarbonyls as the reactions proceeded. In each experiment, a series of intermittent irradiations was carried out with analysis of reactants and products during the intervening dark periods. The total irradiation times, at 20% of the maximum light intensity, ranged up to 100 min for each *n*-alkane resulting in consumption of up to 28% (*n*-pentane), 42% (*n*-hexane), 49% (*n*-heptane) and 57%

(*n*-octane) of the initially present alkane. The extents of reaction were limited by photolytic depletion of methyl nitrite, which resulted in decreasing OH radical concentrations with irradiation time [12]. 3-Pentanone, at a concentration of ~ (7–8) × 10¹² molecule cm⁻³, was monitored in the chamber during the experiments to ensure that the derivatization efficiency did not decrease appreciably.

For the analysis of the *n*-alkanes *n*-hexane through *n*-octane and the 3-pentanone internal standard, 100 cm³ gas samples were collected from the chamber onto Tenax-TA solid adsorbent with subsequent thermal desorption at ~250 °C onto a 30 m DB-1701 megabore column held at -40 °C and then temperature programmed to 200 °C at 8 °C min⁻¹. Analyses of *n*-pentane were carried out with gas samples being collected in a 100 cm³ all-glass, gas-tight syringe and introduced via a gas sampling loop onto a 30 m DB-5 megabore column initially held at -25 °C, and then temperature programmed to 200 °C at 8 °C min⁻¹.

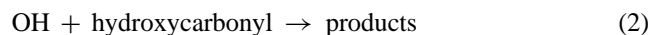
Carbonyl-containing products were identified by using on-fiber derivatization with SPME [8,9,13–15]. A 65 μm polydimethylsiloxane/divinylbenzene PDMS/DVB fiber was coated with PFBHA hydrochloride [8,14,15]. This involved headspace extraction from 4 ml of an aqueous solution (~170 mg of PFBHA hydrochloride per 100 ml of water) in a 20 ml vial over a 30 min period, with rapid agitation using a magnetic stirrer. The PFBHA coating of the fiber was carried out under nitrogen gas to minimize any acetone contamination from laboratory air. The coated fiber was then exposed to the reactants in the chamber for 5 min to form a PFBHA-carbonyl oxime [14]. For GC-FID analyses of the hydroxycarbonyl- and 3-pentanone-oximes, the exposed fiber was removed from the chamber and thermally desorbed for 2 min (injection port temperature at 250 °C) onto a 30 m DB-1, 0.32 mm i.d., capillary column (3 μm phase thickness) held at 40 °C and then temperature programmed at 20 °C min⁻¹ to 160 °C, then at 2 °C min⁻¹ to 240 °C and then at 20 °C min⁻¹ to 300 °C.

The following chemicals, with their stated purities, were used: *n*-pentane (99+%), *n*-hexane (99+%), *n*-octane (99+%) and 3-pentanone (99+%), Aldrich Chemical Company; *n*-heptane (99+%), Mallinckrodt; NO (≥99.0%), Matheson Gas Products. Methyl nitrite was prepared as described by Taylor et al. [16] and stored at 77 K under vacuum.

3. Results

Using gas chromatography-mass spectrometry for isomer-specific identifications, the 1,4-hydroxycarbonyl products formed from the OH radical-initiated reactions of *n*-pentane through *n*-octane have previously been reported from this laboratory [8]. Our present 1,4-hydroxycarbonyl assignments are based on this earlier work [8] and here we monitored their relative concentrations, as oxime derivatives, by GC-FID. The approach used [15] was to gen-

erate the 1,4-hydroxycarbonyls from their parent *n*-alkane and monitor, on a relative basis, the concentrations of the 1,4-hydroxycarbonyls as a function of the extent of reaction of the alkane, defined as $\ln([\text{alkane}]_{t_0}/[\text{alkane}]_t)$, where $[\text{alkane}]_{t_0}$ and $[\text{alkane}]_t$ are the alkane concentrations at time t_0 and t , respectively. For the reactions,



then,

$$[\text{hydroxycarbonyl}]_t = \frac{\alpha[\text{alkane}]_{t_0}k_1}{k_2 - k_1} (e^{-k_1[\text{OH}]t} - e^{-k_2[\text{OH}]t}) \quad (I)$$

where α is the hydroxycarbonyl yield from reaction (1), k_1 and k_2 are the rate constants for reactions (1) and (2), respectively, $[\text{hydroxycarbonyl}]_t$ is the hydroxycarbonyl concentration at time t , $[\text{alkane}]_{t_0}$ is the initial *n*-alkane concentration and $[\text{OH}]$ is the OH radical concentration. Computer calculations show that Eq. (I) holds even if the OH radical concentration is not constant (in which case $[\text{OH}]_t$ is replaced by $\int[\text{OH}]dt$) [15]. The sole assumption for formulating Eq. (I) is that reactions (1) and (2) are the only loss processes for the alkane and the hydroxycarbonyl, respectively. Because $\ln([\text{alkane}]_{t_0}/[\text{alkane}]_t) = k_1 \int[\text{OH}]dt$ (or $k_1[\text{OH}]t$ if the OH radical concentration is constant), then Eq. (I) becomes

$$[\text{hydroxycarbonyl}]_t = A(e^{-x} - e^{-Bx}) \quad (II)$$

where $A = \alpha[\text{alkane}]_{t_0}k_1/(k_2 - k_1)$, $B = k_2/k_1$ and $x = \ln([\text{alkane}]_{t_0}/[\text{alkane}]_t)$. For a given experiment, or a series of experiments with the same initial concentration of the same alkane, A is therefore constant, and the hydroxycarbonyl concentration at time t depends on the values of x and B . The variation of the hydroxycarbonyl concentration with extent of reaction, $\ln([\text{alkane}]_{t_0}/[\text{alkane}]_t)$, depends on the hydroxycarbonyl formation yield, α , and the rate constant ratio k_2/k_1 [15]. The value of $\ln([\text{alkane}]_{t_0}/[\text{alkane}]_t)$ at which the hydroxycarbonyl concentration is a maximum ($[\text{hydroxycarbonyl}]_{\text{max}}$) depends only on the rate constant ratio k_2/k_1 and is given by $\ln(k_2/k_1)/[(k_2/k_1) - 1] = \ln B/(B - 1)$ [15]. Measurement of the hydroxycarbonyl concentration as a function of the extent of reaction during OH radical-initiated reactions of the precursor *n*-alkane should then allow the rate constant ratio k_2/k_1 , and hence the rate constant k_2 , to be determined.

A series of $\text{CH}_3\text{ONO}-\text{NO}-n\text{-alkane}$ -air irradiations were carried out. The formation yields of the 4-hydroxyaldehydes from these reactions are small [8] and the GC-FID peaks of their oximes could not be unequivocally identified and therefore no data are reported here concerning the kinetics of their OH radical reactions. The oximes of the 1,4-hydroxycarbonyls exist as *Z*- and *E*-isomers, with the ratio of the two isomer peaks being constant and characteristic for a particular 1,4-hydroxycarbonyl. Therefore, for each of the 1,4-hydroxyketones, one or both of the GC peaks of the

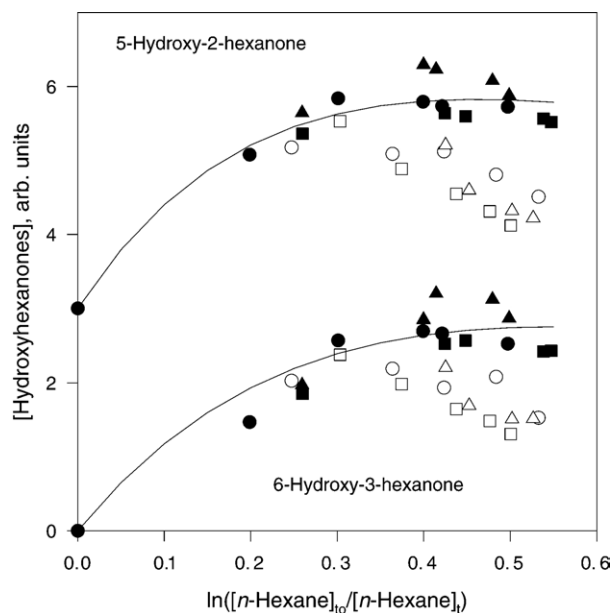


Fig. 1. Plots of Eq. (II) for formation of 6-hydroxy-3-hexanone and 5-hydroxy-2-hexanone from the OH radical-initiated reaction of *n*-hexane at $\leq 5\%$ relative humidity (open symbols) and at $50 \pm 3\%$ relative humidity (filled symbols). The lines are calculated from Eq. (II) using rate constant ratios $k_2/k_1 = 3.0$ for 6-hydroxy-3-hexanone and 4.0 for 5-hydroxy-2-hexanone. At each relative humidity, the different symbols denote different experiments, and the hydroxycarbonyl concentrations are in arbitrary units based on the GC peak areas. The data for 5-hydroxy-2-hexanone have been displaced vertically by 3.0 units for clarity.

Z- and *E*-oximes was used to monitor the concentration of the 1,4-hydroxyketones during the reactions, using only GC peaks that were not interfered with by other GC peaks. For example, while one oxime from 5-hydroxy-2-octanone co-elutes with one oxime from 6-hydroxy-3-octanone [8], the non-overlapping oxime peaks could be utilized to investigate the kinetics of the OH radical reactions with these two hydroxyoctanones.

Initial experiments involved the OH radical-initiated reaction of *n*-hexane at $\leq 5\%$ relative humidity, and the GC peak areas of the oximes of 6-hydroxy-3-hexanone and 5-hydroxy-2-hexanone are plotted against the extent of reaction of *n*-hexane in Fig. 1 (open symbols), with the different experiments being shown by different symbols. Here, as in Figs. 2–5, the GC-FID peak areas of the oximes of the 1,4-hydroxyketones have been scaled to a constant initial concentration of the *n*-alkane [15]. As noted above, the OH radical concentration decreases with irradiation time [12] because of depletion of methyl nitrite, leading to rapidly decreasing incremental changes in $\ln([\text{alkane}]_{t_0}/[\text{alkane}]_t)$ with successive irradiation periods. As the extent of reaction increased the OH radical concentrations decreased, and any dark losses of the hydroxycarbonyls therefore became evident because the dark losses during the 50–55 min time periods between consecutive analyses became competitive with the OH radical reaction. Attempts to fit the 6-hydroxy-3-hexanone and 5-hydroxy-2-hexanone data obtained at $\leq 5\%$ relative humidity

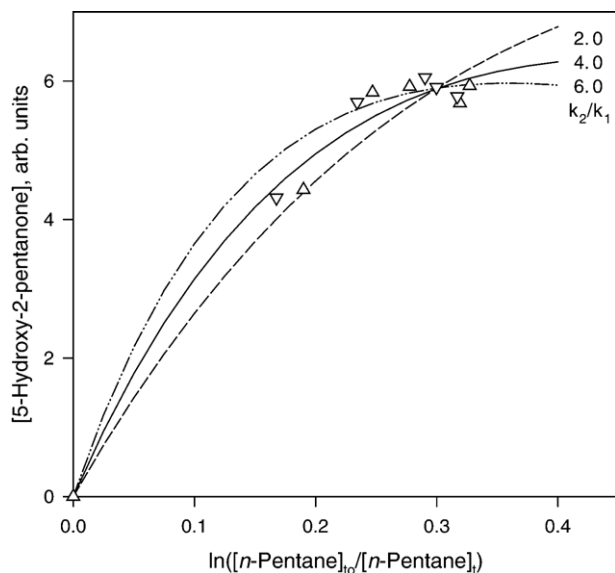


Fig. 2. Plot of Eq. (II) for formation of 5-hydroxy-2-pentanone from the OH radical-initiated reaction of *n*-pentane at $49 \pm 4\%$ relative humidity, together with calculated fits to Eq. (II) for the rate constant ratios noted. The different symbols denote different experiments, and the 5-hydroxy-2-pentanone concentrations are in arbitrary units based on the GC peak areas.

with Eq. (II) indicated that the hydroxyketone concentrations decreased much more rapidly when $\ln([n\text{-hexane}]_{t_0}/[n\text{-hexane}]_t)$ exceeded 0.3 than expected, as evident from the fits shown in Fig. 1 (see also below). This could be due to 6-hydroxy-3-hexanone and 5-hydroxy-2-hexanone undergo-

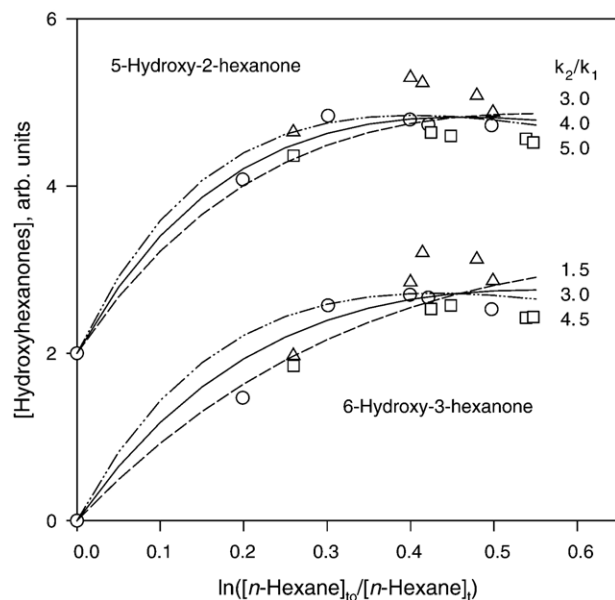


Fig. 3. Plots of Eq. (II) for formation of 6-hydroxy-3-hexanone and 5-hydroxy-2-hexanone from the OH radical-initiated reaction of *n*-hexane at $50 \pm 3\%$ relative humidity, together with calculated fits to Eq. (II) for the rate constant ratios noted. The different symbols denote different experiments, and the hydroxycarbonyl concentrations are in arbitrary units based on the GC peak areas. The data for 5-hydroxy-2-hexanone have been displaced vertically by 2.0 units for clarity.

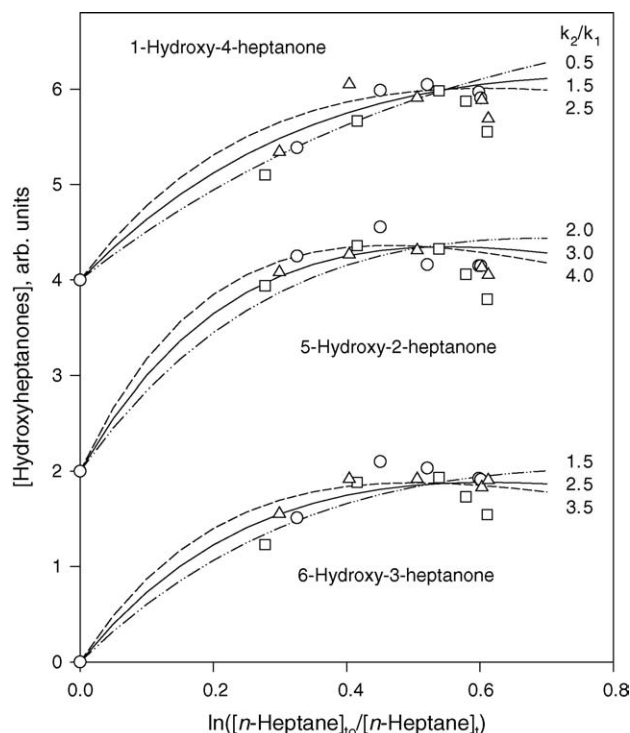
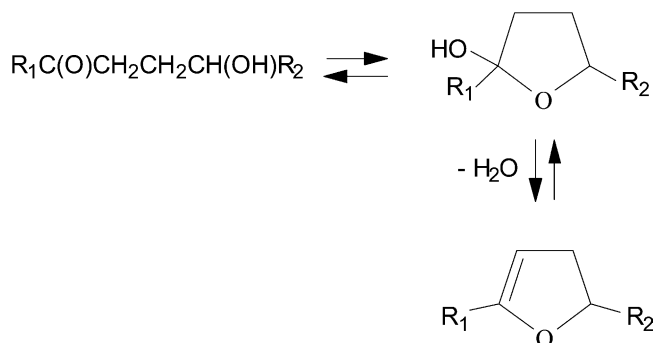


Fig. 4. Plots of Eq. (II) for formation of 6-hydroxy-3-heptanone, 5-hydroxy-2-heptanone and 1-hydroxy-4-heptanone from the OH radical-initiated reaction of *n*-heptane at $50 \pm 5\%$ relative humidity, together with calculated fits to Eq. (II) for the rate constant ratios noted. The different symbols denote different experiments, and the hydroxycarbonyl concentrations are in arbitrary units based on the GC peak areas. The data for 5-hydroxy-2-heptanone and 1-hydroxy-4-heptanone have been displaced vertically by 2.0 and 4.0 units, respectively, for clarity.

ing cyclization, with loss of water, to form 4,5-dihydro-2-ethylfuran and 4,5-dihydro-2,5-dimethylfuran, respectively, as previously observed for 5-hydroxy-2-pentanone under dry conditions [10,11]. The reactions thought to be involved are as follows, and appear to occur in the gas phase [11].



Accordingly, we carried out analogous experiments at $\sim 50\%$ relative humidity, and these data are also plotted in Fig. 1 (filled symbols). While there may still be some decrease in the 6-hydroxy-3-hexanone and 5-hydroxy-2-hexanone concentrations at longer reaction times over that predicted from use of Eq. (II), the effect is much reduced. It therefore appears that these two hydroxyhexanones undergo

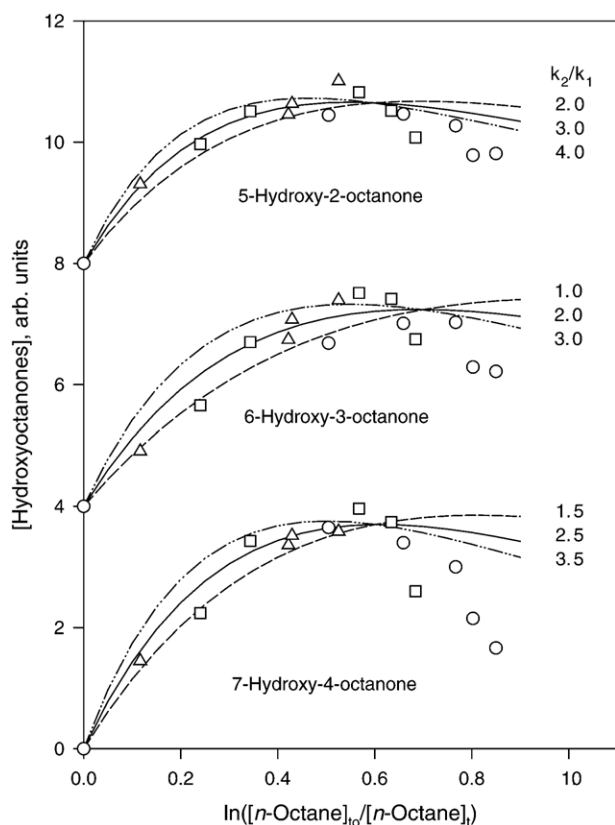


Fig. 5. Plots of Eq. (II) for formation of 7-hydroxy-4-octanone, 6-hydroxy-3-octanone and 5-hydroxy-2-octanone from the OH radical-initiated reaction of *n*-octane at $47 \pm 1\%$ relative humidity, together with calculated fits to Eq. (II) for the rate constant ratios noted. The different symbols denote different experiments, and the hydroxycarbonyl concentrations are in arbitrary units based on the GC peak areas. The data for 6-hydroxy-3-octanone and 5-hydroxy-2-octanone have been displaced vertically by 4.0 and 8.0 units, respectively, for clarity.

cyclization with loss of water to form the dihydrofurans at low water vapor concentrations, but that this occurs to a much lesser extent at $\sim 50\%$ relative humidity. All further experiments were therefore carried out at $50 \pm 5\%$ relative humidity.

Data obtained from $\text{CH}_3\text{ONO}-\text{NO}$ -air irradiations of *n*-pentane, *n*-hexane, *n*-heptane and *n*-octane are plotted in Figs. 2–5, respectively, in the form of the GC peak areas of one or both of the oxime(s) of the 1,4-hydroxyketones formed from these reactions against the extent of reaction. Also shown in these Figures are calculated curves obtained from Eq. (II) at various values of k_2/k_1 ($=B$) which appear to encompass the data (the calculated hydroxyketone concentration has been scaled in the *Y*-direction to fit the experimental data in each case). While there is a certain amount of run-to-run variability, mainly showing up as variability in the GC peak areas of the oximes, for a given hydroxyketone the shapes of the curves are very similar from run to run. As noted above, 5-hydroxy-2-pentanone was purchased and its the rate constant k_2 measured relative to that for 4-methyl-

2-pentanone [9]. Because of the limited extent of reaction which could be achieved for *n*-pentane (insufficient to unambiguously define the value of $\ln([n\text{-pentane}]_{t_0}/[n\text{-pentane}]_t)$ at which [5-hydroxy-2-pentanone] maximizes), only a brief study of this reaction was carried out to check whether or not the experimental approach used here would give a rate constant ratio k_2/k_1 in agreement with our previous measurement of k_2 [9]. As seen in Table 1, the rate constant obtained in this work agrees with the more precise direct measurement [9].

Even at 50% relative humidity, some of the hydroxyketones appear to decrease more rapidly than expected from only OH radical reaction [i.e., from reactions (1) and (2) only, in accordance with Eqs. (I) and (II)], suggesting that these hydroxyketones are undergoing cyclization with loss of water to form alkyl-substituted 4,5-dihydrofurans to greater or lesser extents. This is particularly apparent for all three hydroxyoctanones (Fig. 5). 1-Hydroxy-4-heptanone and 5-hydroxy-2-heptanone (Fig. 4) also show some evidence for a consistent decrease in concentration during the last 50–110 min of the experiments. A study of the dark behavior of 1,4-hydroxycarbonyls as a function of relative humidity is reported elsewhere [17].

Table 1 lists the rate constant ratios k_2/k_1 derived from the comparisons of the experimental data with the calculated curves based on Eq. (II), and shown in Figs. 2–5. The derived rate constant ratios are subject to significant uncertainties, in part because only limited extents of reaction could be achieved with the experimental conditions used, and for the hydroxyketones formed in the *n*-heptane and *n*-octane reactions, because of the dark reactions of the hydroxyketones to form unsaturated cyclized products (see above and [17]). These rate constant ratios have been placed on an absolute basis using rate constants k_1 for the reactions of OH radicals with *n*-alkanes at 298 K (in units of $10^{-12} \text{ cm}^3 \text{ molecule}^{-1} \text{ s}^{-1}$) of: *n*-pentane, 3.80; *n*-hexane, 5.20; *n*-heptane, 6.76; *n*-octane, 8.11 [3], and the resulting rate constants k_2 are also given in Table 1. The rate constants k_2 estimated as described by Kwok and Atkinson [18], as revised by Bethel et al. [19], are shown in Table 1 for comparison together with the measured rate constant of Aschmann et al. [9] for 5-hydroxy-2-pentanone. Taking 5-hydroxy-2-hexanone as the example, the estimation method of Kwok and Atkinson [18] considers H-atom abstraction from the various CH_3 (k_{prim}), CH_2 (k_{sec}) and CH (k_{tert}) groups and from the OH group (k_{OH}), with the effects of substituent groups “X” at the α and, in some cases, the β positions to the CH_3 , CH_2 and CH groups being taken into account by means of substituent factors $F(X)$ [18]. The rate constant for 5-hydroxy-2-hexanone is then calculated from $k(\text{OH} + \text{CH}_3\text{C}(\text{O})\text{CH}_2\text{CH}_2\text{CH}(\text{OH})\text{CH}_3) = \{k_{\text{prim}}F(>\text{C}=\text{O}) + k_{\text{sec}}F(>\text{C}=\text{O})F(-\text{CH}_2-) + k_{\text{sec}}F(-\text{CH}_2\text{C}(\text{O})-)F(-\text{CH}(\text{OH})-) + k_{\text{tert}}F(-\text{CH}_2-)F(-\text{OH})F(-\text{CH}_3) + k_{\text{OH}} + k_{\text{prim}}F(-\text{CH}(\text{OH})-)\}$. At 298 K, the partial rate constants are $k_{\text{prim}} = 1.36 \times 10^{-13} \text{ cm}^3 \text{ molecule}^{-1} \text{ s}^{-1}$, $k_{\text{sec}} = 9.34 \times 10^{-13} \text{ cm}^3 \text{ molecule}^{-1} \text{ s}^{-1}$, $k_{\text{tert}} = 1.94 \times 10^{-12} \text{ cm}^3 \text{ molecule}^{-1} \text{ s}^{-1}$

Table 1

Rate constants ratios k_2/k_1 and rate constants k_2 for the reactions of OH radicals with 1,4-hydroxycarbonyls, together with estimated rate constants and the measured rate constant for 5-hydroxy-2-pentanone

Alkane	1,4-Hydroxycarbonyl	k_2/k_1	$10^{12} \times k_2$ (cm ³ molecule ⁻¹ s ⁻¹)	
		This work ^a	This work ^b	Estimated ^c
<i>n</i> -Pentane	5-Hydroxy-2-pentanone	4 ± 2	15 ± 8	13.9 (16 ± 4) ^d
<i>n</i> -Hexane	5-Hydroxy-2-hexanone	4.0 ± 1	21 ± 6	17.8
	6-Hydroxy-3-hexanone	3.0 ± 1.5	16 ± 8	15.0
<i>n</i> -Heptane	5-Hydroxy-2-heptanone	3.0 ± 1	20 ± 7	21.7
	6-Hydroxy-3-heptanone	2.5 ± 1	17 ± 7	19.0
	1-Hydroxy-4-heptanone	1.5 ± 1	10 ± 7	18.5
<i>n</i> -Octane	5-Hydroxy-2-octanone	3.0 ± 1	24 ± 9	23.4
	6-Hydroxy-3-octanone	2.0 ± 1	16 ± 9	22.8
	7-Hydroxy-4-octanone	2.5 ± 1	20 ± 9	22.4

^a From comparison of the fits of Eq. (II) with the experimental data shown in Figs. 2–5. For each 1,4-hydroxyketone, the central value of the rate constant ratio is the solid “best-fit” line, while the upper and lower limits to the rate constant ratios set by the cited uncertainties correspond to the dashed and dot–dot–dash lines in Figs. 2–5, which encompass the experimental data during the initial extents of reaction. The occurrence of the dark loss reactions of the hydroxyheptanones and hydroxyoctanones (Figs. 4 and 5) could result in the fitted values of k_2/k_1 being slightly overestimated and hence the rate constant ratios for these compounds may be upper limits. The uncertainties are based on comparison of the calculated curves shown in these figures with the experimental data, and are subjective.

^b Placed on an absolute basis using rate constants k_1 for the reactions of OH radicals with *n*-alkanes at 298 K (in units of 10⁻¹² cm³ molecule⁻¹ s⁻¹) of: *n*-pentane, 3.80; *n*-hexane, 5.20; *n*-heptane, 6.76; *n*-octane, 8.11 [3]. Uncertainties in the rate constants k_1 (~±10%) are small compared to the uncertainties in the rate constant ratios k_2/k_1 and have been neglected.

^c Rate constants for the reactions of OH radicals with the 1,4-hydroxyketones were calculated using the method described by Kwok and Atkinson [18], as revised by Bethel et al. [19].

^d Rate constant measured by Aschmann et al. [9].

and $k_{OH} = 1.4 \times 10^{-13}$ cm³ molecule⁻¹ s⁻¹ [18], and the necessary group substituent factors are $F(>C=O) = 0.75$, $F(-CH_2-) = 1.23$, $F(-CH_2C(O)-) = 3.9$, $F(-CH(OH)-) = 2.6$, $F(-OH) = 2.9$ and $F(-CH_3) = 1.0$ [18,19]. This results in the estimated rate constant for 5-hydroxy-2-hexanone given in Table 1.

The agreement between the rate constants k_2 measured in this work and the values estimated using the structure–reactivity method of Kwok and Atkinson [18] and Bethel et al. [19] is surprisingly good, with the major discrepancy being for 1-hydroxy-4-heptanone (Table 1). Furthermore, the present rate constant for 5-hydroxy-2-pentanone, despite its large uncertainty, is consistent with the value recently measured more directly by Aschmann et al. [9], suggesting that the present experimental method can provide valuable kinetic data for compounds which are not commercially available. However, given the significant uncertainties in the rate constant ratios k_2/k_1 derived here, we suggest that the values estimated using the method of Kwok et al. [18] (as revised by Bethel et al. [19]) be used for the 1,4-hydroxyketones studied here, and for other 1,4-hydroxyketones for which experimental data are not available.

Acknowledgements

The authors gratefully thank the National Science Foundation (Grant No. ATM-0234586) for supporting this research. While this research has been supported by this Agency, it has not been reviewed by this Agency and no official endorsement should be inferred.

References

- [1] S.K. Hoekman, Environ. Sci. Technol. 26 (1992) 1206–1216.
- [2] J.G. Calvert, R. Atkinson, K.H. Becker, R.M. Kamens, J.H. Seinfeld, T.J. Wallington, G. Yarwood, The Mechanisms of Atmospheric Photooxidation of Aromatic Hydrocarbons, Oxford University Press, New York, 2002.
- [3] R. Atkinson, J. Arey, Chem. Rev. 103 (2003) 4605–4638.
- [4] J. Eberhard, C. Müller, D.W. Stocker, J.A. Kerr, Environ. Sci. Technol. 29 (1995) 232–241.
- [5] R. Atkinson, E.S.C. Kwok, J. Arey, S.M. Aschmann, Faraday Discuss. 100 (1995) 23–37.
- [6] E.S.C. Kwok, J. Arey, R. Atkinson, J. Phys. Chem. 100 (1996) 214–219.
- [7] J. Arey, S.M. Aschmann, E.S.C. Kwok, R. Atkinson, J. Phys. Chem. A 105 (2001) 1020–1027.
- [8] F. Reisen, S.M. Aschmann, R. Atkinson, J. Arey, Environ. Sci. Technol. 39 (2005) 4447–4453.
- [9] S.M. Aschmann, J. Arey, R. Atkinson, J. Atmos. Chem. 45 (2003) 289–299.
- [10] F. Cavalli, I. Barnes, K.H. Becker, Environ. Sci. Technol. 34 (2000) 4111–4116.
- [11] P. Martin, E.C. Tuazon, S.M. Aschmann, J. Arey, R. Atkinson, J. Phys. Chem. A 106 (2002) 11492–11501.
- [12] R. Atkinson, W.P.L. Carter, A.M. Winer, J.N. Pitts Jr., J. Air Pollut. Control Assoc. 31 (1981) 1090–1092.
- [13] H.L. Bethel, R. Atkinson, J. Arey, J. Phys. Chem. A 107 (2003) 6200–6205.
- [14] F. Reisen, S.M. Aschmann, R. Atkinson, J. Arey, Environ. Sci. Technol. 37 (2003) 4664–4671.
- [15] J. Baker, J. Arey, R. Atkinson, J. Phys. Chem. A 108 (2004) 7032–7037.
- [16] W.D. Taylor, T.D. Allston, M.J. Moscato, G.B. Fazekas, R. Kozlowski, G.A. Takacs, Int. J. Chem. Kinet. 12 (1980) 231–240.
- [17] T. Holt, R. Atkinson, J. Arey, J. Photochem. Photobiol. A: Chem., submitted for publication.
- [18] E.S.C. Kwok, R. Atkinson, Atmos. Environ. 29 (1995) 1685–1695.
- [19] H.L. Bethel, R. Atkinson, J. Arey, Int. J. Chem. Kinet. 33 (2001) 310–316.